Development 134, 4491-4501 (2007) doi:10.1242/dev.011452

Semaphorin and neuropilin co-expression in motoneurons sets axon sensitivity to environmental semaphorin sources during motor axon pathfinding

Frédéric Moret, Christelle Renaudot, Muriel Bozon and Valérie Castellani*

Class III semaphorins (SemaIIIs) are intercellular cues secreted by surrounding tissues to guide migrating cells and axons in the developing organism. This chemotropic activity is crucial for the formation of nerves and vasculature. Intriguingly, SemaIIIs are also synthesized by neurons during axon pathfinding, but their function as intrinsic cues remains unknown. We have explored the role of Sema3A expression in motoneurons during spinal nerve development. Loss- and gain-of-function in the neural tube of the chick embryo were undertaken to target Sema3A expression in motoneurons while preserving Sema3A sources localized in peripheral tissues, known to provide important repulsive information for delineating the routes of motor axons towards their ventral or dorsal targets. Strikingly, Sema3A overexpression induced defasciculation and exuberant growth of motor axon projections into these normally non-permissive territories. Moreover, knockdown studies showed that motoneuronal Sema3A is required for correct spinal nerve compaction and dorsal motor axon extension. Further analysis of Sema3A gain- and loss-of-function in ex vivo models revealed that Sema3A in motoneurons sets the level of sensitivity of their growth cones to exogenous Sema3A exposure. This regulation is associated with post-transcriptional and local control of the availability of the Sema3A receptor neuropilin 1 at the growth cone surface. Thus, by modulating the strength of Sema3A-mediated environmental repulsive constraints, Sema3A in motoneurons enables axons to extend more or less far away from these repulsive sources. Such interplay between intrinsic and extrinsic Sema3A may represent a fundamental mechanism in the accurate specification of axon pathways.

KEY WORDS: Semaphorin, Motoneuron, Axon guidance

INTRODUCTION

Mechanisms underlying the wiring of neuronal connectivity remain puzzling with regard to the limited repertoire of guidance cues used to achieve the tremendous diversity of axon pathways. Tight spatiotemporal regulation of both ligands and receptors, together with the capacity of neuronal growth cones to vary their response to guidance cues between attraction and repulsion are probably critical in the diversification of pathway choices (Yu and Bargmann, 2001). However, other types of regulation might exist which amplify the repertoire of guidance decisions and control their temporal and spatial accuracy. Highly potent mechanisms are those that would modulate the strength of the effects elicited by guidance cues by setting distinct levels of sensitivity, thus controlling the amplitude of axon re-orientation induced by guidance sources. However, the contribution of such mechanisms in axon navigation remains poorly explored. Class III secreted semaphorins (SemaIIIs) is a group of seven widely expressed chemotropic factors, from Sema3A to Sema3G, with repulsive and attractive activities (Raper, 2000). Loss-of-function approaches in mice provided evidence for important roles of SemaIIIs and their receptors, the neuropilins, in patterning neuronal connections in various regions of the developing organism (Raper, 2000). Likewise in the motor system, peripheral expression of repulsive SemaIIIs in the dermamyotome, the notochord, the ectoderm and the limb was demonstrated to provide surrounding repulsive forces to constrain spinal nerve fasciculation and trajectory towards muscle targets (Behar et al., 1996; Huber et al., 2005; Kitsukawa et al., 1997; Raper, 2000; Taniguchi et al., 1997; Varela-Echavarria et al., 1997) (Fig. 1). Intriguingly, mRNAs for several SemaIIIs, including Sema3A, are also strongly detected in spinal motoneurons by the time their axons elongate and innervate their targets (Luo et al., 1995; Puschel et al., 1995), which appears to be inconsistent with a chemotropic effect on motor growth cones. Other studies also described complex patterns of SemaIIIs in cranial motoneurons (Chilton and Guthrie, 2003; Melendez-Herrera and Varela-Echavarria, 2006). We hypothesized that this intrinsic source of Sema3A could participate in the guidance of motor axons through a non-classical modality, and that this contribution could have been so far disregarded due to limitations of knockout strategies removing both intrinsic and environmentally expressed Sema3A. We addressed this issue by selective manipulation of Sema3A expression in spinal motoneurons of the chick embryos. We report here an unexpected mechanism for chemotropic cues by which Sema3A in motoneurons sets the sensitivity of their growth cones to environmental sources of Sema3A by locally controlling the availability of the Sema3A receptor neuropilin 1 at the growth cone surface. Our data also show that differential levels of Sema3A in populations of motoneurons connecting different targets is crucial for appropriate organization of their axon pathways.

Université de Lyon, F-69003, France, Université Lyon1, F-69003, France. CNRS, UMR5534, Centre de Génétique Moléculaire et Cellulaire, Villeurbanne, F-69622, France.

*Author for correspondence (e-mail: castellani@cgmc.univ-lyon1.fr)

Accepted 19 September 2007

MATERIALS AND METHODS

Plasmid construction

Sema3AiresEGFP bicistronic construct was derived from pAG-NT-Coll1 plasmid [kindly provided by J. Raper (Feiner et al., 1997)]. An iresEGFP fragment was amplified from ires2EGFP plasmid (Clontech, Mountain View, USA) by PCR between suitable primers, then inserted at the *Xho*I site located downstream from the chick Sema3A cDNA.

For RNA interference experiments, oligoduplexes based on the following sequences: 5′-GGAAGCACCTACAAGAGAATTCAAGAGATTCTCTT-GTAGGTGCTTCCACTTTTTT-3′; 5′-GACACCCATATCTCTTCCTTT-CAAGAGAAGGAAGAGATATGGGTGTCTTTTTT-3′ for pShSema3A, and pShScramble, respectively, were inserted in the pSilencer-U6-1.0 (Ambion, Huntingdon, UK) between the *Apa*I and *Eco*RI sites. A fragment containing the EGFP cDNA downstream from a CMV promoter, terminated by a SV40 polyadenylation site and flanked by *Nsi*I and *Not*I restriction sites was obtained after digestion of the pEGFP-N1 plasmid (Clontech) and then inserted between *Pst*I and *Not*I sites within the pSilencerU6 vector.

In ovo electroporation

In ovo electroporation of chick embryos (*Gallus gallus*; EARL Morizeau, Dangers, France) was performed as described previously (Creuzet et al., 2002). The constructs were introduced into the neural tube at the cervical and brachial levels either in stage HH14 embryos, or in HH15-16 embryos (Hamburger and Hamilton, 1992) to avoid plasmid expression in dorsal root ganglia. Plasmids prepared with the EndoFree Maxiprep Kit (Macherey-Nagel, Düren, Germany) were routinely diluted at 1.5 μg/μl in PBS, and at 2 μg/μl for high level Sema3A overexpression.

Histological analyses

20 μm cryosections were obtained from embryos fixed in 4% paraformaldehyde, and embedded in 7.5% gelatine-15% sucrose. Alternatively, 150 μm vibratome sections were used for confocal analysis. In situ hybridization was performed as described previously (Moret et al., 2004). For immunostaining, cryosections, vibratome sections, embryos or explants were incubated overnight with the following antibodies diluted in 2% bovine serum albumin blocking solution: mouse anti-Myc (1/100; 9E10; Sigma, USA), goat anti-neuropilin 1 (1/50; R&D Systems, Minneapolis, USA), mouse anti-neurofilament 160 kDa (NF160kD; 1/100; RMO-270; Zymed, San Francisco, USA). Mouse anti-NgCAM (1/500, 8D9 developed by Dr Vance Lemmon), mouse anti-Islet1/2 (1/100; 39.5D5 developed by Dr Thomas Jessell) and mouse anti-P0 (1/100; 1E8 developed by Dr Erick Frank) were obtained from the Developmental Studies Hybridoma Bank developed under the auspices of the NIHCD and maintained by the University of Iowa (Department of Biological Sciences, Iowa City, USA). For chromogenic immunostaining, suitable biotinylated antibodies, then the ABC complex (Vectastain), were used prior to DAB staining (Vector, Paris, France).

For immunofluorescent staining, sections were incubated with Alexa Fluor 594 antibodies (1:1000; Molecular Probes) or Fluoprobes 546 antibodies.

Nrp1 and NgCAM immunofluorescent labeling on explants, either non-permeabilized or permeabilized with 0.05% Triton X-100, were detected with combined suitable Alexa Fluor 594 (1/200) and biotinylated antibodies (1/100). Explants were subsequently incubated with Alexa Fluor 350-streptavidin (1/100; Molecular Probes).

TdT-mediated dUTP nick end labeling (TUNEL) was performed as described previously (Gavrieli et al., 1992) and revealed using the ABC complex.

Explant cultures

The ventral third of spinal cords was dissected out from Hamburger and Hamilton (HH) stage 23-24 chick embryos at the brachial level in HBSS-glucose 1%. Explants were cultured on glass coverslips precoated with poly-ornithin (10 μg/ml, Sigma) and laminin (50 μg/ml, Sigma), and grown in a complete medium as previously described (Marthiens et al., 2005). Immunolabeling using the motoneuron-specific axonal marker NgCAM confirmed that fibers extending from these explants were motoneuron axons.

Collapse assays

Conditioned media were obtained by transfection of Sema3AiresEGFP or control constructs in human kidney epithelial cells (HEK 293-T) using Exgen (Euromedex, Les Ulys, France), cultured in DMEM medium with 10% heat-inactivated FBS, 0.05% penicillin, streptomycin, 1% amphotericinB. After 24 hours in culture at 37°C, ventral spinal cord explants were incubated with control and Sema supernatants for 30 minutes at 37°C, and fixed in 4% paraformaldehyde. Individual axons were randomly selected under phase-contrast microscopy and their morphology examined at 40× magnification as described by Falk et al. (Falk et al., 2005). A minimum of three independent experiments were used for each analysis, excepted for those shown in Fig. 4C in which each condition was performed in duplicate within the same experiment.

Microscopy and fluorescence quantification

Labeling was examined under an Axiovert microscope (Zeiss, Germany) equipped with a Coolsnap CCD camera (Photometrics, Evry, France) or a LSM510 Meta confocal microscope (Zeiss). Fluorescence was quantified with ImageJ software (National Institutes of Health, USA). For quantification of the spinal nerve thickness, NgCAM immunofluorescent staining was performed on horizontal sections across spinal nerves. Images were captured at 10× magnification. The spinal nerve outline was traced on NgCAM labeling and its surface measured. Normalized area reported on the histogram was defined as the quotient of nerve section areas between electroporated and non-electroporated sides. For quantification of medial motor column (MMCm) axon length, transverse sections were immunostained with NF160kD. The length of motor axons from the ventral horn exit point to the terminal tip was measured. The normalized length reported in the histogram was defined as the quotient between the longest EGFP-positive ($EGFP^+$) fiber and the longest neurofilament (NF)-positive and EGFP-negative ($NF^+/EGFP^-$) axon in each dorsal ramus. For quantification of growth cone fluorescence, images were captured at 40× magnification with constant exposure parameters below pixel saturation. Growth cone outline was traced with NgCAM staining, which clearly delineated filopodia and lamellipodia in both control and experimental conditions. After background subtraction, the intensity of Nrp1 and NgCAM staining was measured within the outline, and the mean intensity per pixel was calculated. Intensity values were normalized to the respective control experiments. Four independent experiments were performed using a minimum of 20 explants from five embryos for each construct.

Statistical analysis

Statistical analyses were carried out using the Student's *t*-test or χ^2 test for collapse assays and Mann-Whitney test for immunofluorescence quantifications.

RESULTS

Dynamic and differential Sema3A expression in spinal motoneuron columns

To assess the role of Sema3A in motoneurons, we first carefully examined its expression during spinal motoneuron development. Sema3A is differentially and dynamically expressed among spinal motoneurons (Fig. 1). It is detected in Lim3-positive motoneurons of the medial motor column (MMC) both at brachial and thoracic levels, by the time their axons extend between the dermamyotome and the dorsal root ganglion (DRG) to form the dorsal ramus (Fig. 1A). Sema3A expression is not detected in neurons of the lateral motor column (LMC) when their axons elongate ventrally between the notochord and the dermamyotome (Fig. 1A) but is activated when they reach the base of the limb (Fig. 1A,B). By contrast, both populations of motoneurons express the Sema3A receptor Nrp1 and are competent to respond to peripheral repulsive sources of the cue (Fig. 1A) (Varela-Echavarria et al., 1997). Thus differential intrinsic Sema3A expression discriminates motoneuron populations projecting along ventral and dorsal routes.

Premature expression of Sema3A in motoneurons led to dramatic axon guidance defects

To investigate the significance of intrinsic Sema3A expression, gain- and loss-of-function experiments were performed by in ovo electroporation of the chick neural tube, to specifically target spinal but not peripheral Sema3A expression in the motor system (see

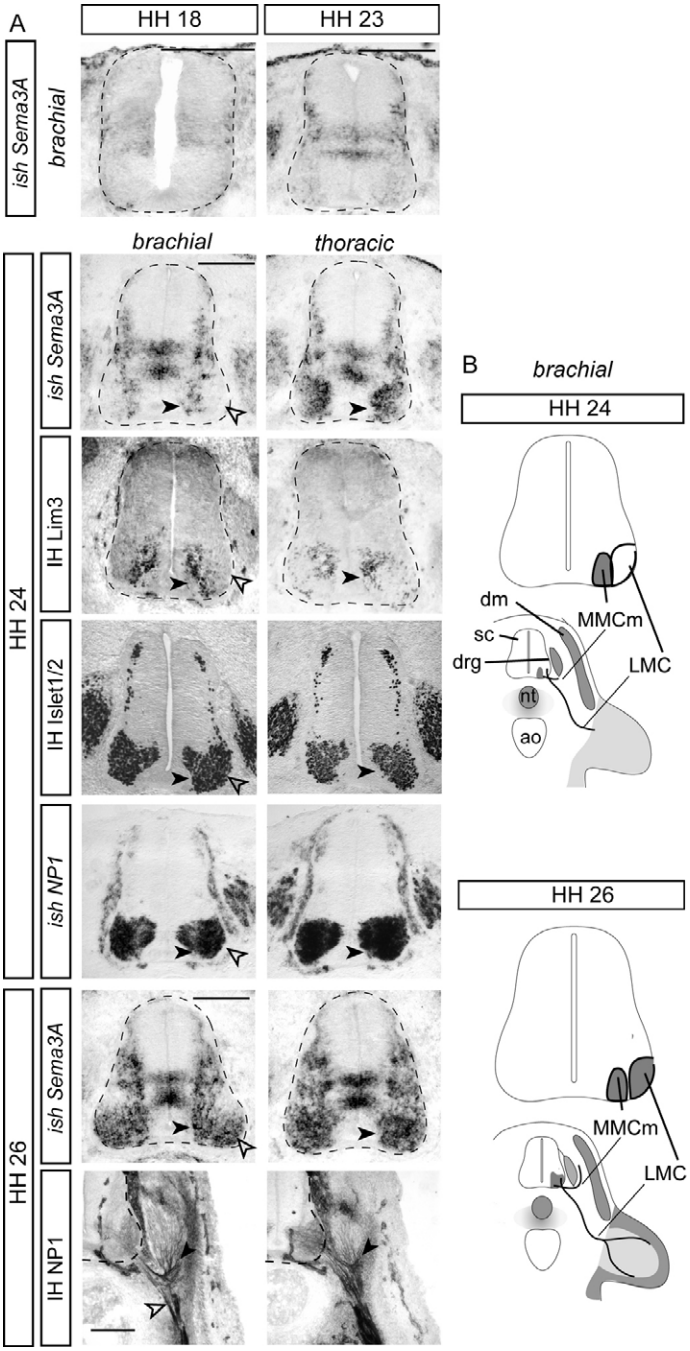

Fig. 1. Sema3A and Nrp1 coexpression in spinal motoneurons. (**A**) In situ hybridization of *Sema3A* mRNA on brachial and thoracic transverse sections of chick spinal cord from HH18-26 embryos. Lim3 and Islet1/2 immunostainings performed on adjacent sections are provided to show that *Sema3A* expression coincides with the medial motor column (MMCm: black arrowhead) and not with the lateral motor column (LMC: white arrowhead) at HH24. In situ hybridization and immunostaining of Nrp1 (NP1) show that both MMCm (black arrowhead) and LMC (white arrowhead) neurons express Nrp1 (NP1). (**B**) Schematic of the Sema3A expression pattern (gray) at HH24 and HH26 in spinal motoneurons and in peripheral tissues, in parallel with motor projections at the brachial level. sc, spinal cord; dm, dermamyotome; drg, dorsal root ganglion; nt, notochord; ao, aorta. Sema3A expression is observed at HH24 in MMCm neurons forming the dorsal ramus, but not in LMC neurons extending to the ventral ramus, and is then expanded at HH25-26 in most motoneurons. Scale bars: 100 μm.

Fig. S1B,C,I in the supplementary material). Sema3A overexpression and vector-based RNAi strategies were designed to specifically label axons of neurons misexpressing Sema3A with EGFP, and projections were analyzed in classical and confocal microscopy. Electroporation of a control EGFP construct in motoneurons did not alter the development of their spinal nerves compared to non-electroporated embryos. By contrast, premature Sema3AiresEGFP expression led to severe defects of motor projections (Fig. 2 and see Table S1 in the supplementary material). The LMC axons projecting along the ventral ramus were strongly defasciculated (Fig. 2A,B) with Sema3AiresEGFP$^+$ fibers split into numerous fascicles (Fig. 2B).

Various path-finding errors were also observed (see Table S1 in the supplementary material). In their proximal part, motor axons in control embryos were channeled within the rostral part of each somite/sclerotome between the dermamyotome and the notochord or the DRG (Fig. 2A-D). By contrast, Sema3AiresEGFP$^+$ axons abnormally extended into the nearby caudal sclerotome (Fig. 2A) and could even invade the dermamyotome (Fig. 2B,C) and the DRG (Fig. 2D), and Sema3AiresEGFP$^+$ axons of the dorsal ramus extended over longer distances (Fig. 2E,F). Furthermore at the cervical and brachial levels, Sema3AiresEGFP$^+$ neurons sent ectopic axons medially towards the aorta, which was in sharp contrast with control cervical and brachial axons that grew far from the notochord and the aorta to project only to lateral structures (see Fig. S1G,H in the supplementary material). Thus, premature expression of Sema3A in the spinal cord led motor axons to defasciculate and to invade territories which they normally avoid (Fig. 2G).

We next examined whether these defects could be due to altered localization or survival of motoneurons. Expression pattern of Islet1/2-positive nuclei in the ventral horn was similar in electroporated and non-electroporated half neural tubes from both Sema3AiresEGFP (see Fig. S1F in the supplementary material) and EGFP embryos (data not shown). Moreover, TUNEL labeling on sections from HH23 embryos [thus prior to the period of endogenous motoneuronal apoptosis (Yaginuma et al., 1996)], showed no induction of apoptotic cell death due to Sema3A overexpression (see Fig. S1E in the supplementary material). Next, we searched for differences in the localization of Schwann cells, as their loss was reported to induce defasciculation of spinal nerves (Lin et al., 2000). Schwann cells were detected by immunostaining at the proximal part of spinal nerves at P0 in both control and Sema3A overexpressing embryos (see Fig. S1F in the supplementary material). Thus neither motoneuron cell death and mispositioning in the ventral horn, nor early deficit of Schwann cell development appeared responsible for the defects induced by intrinsic Sema3A overexpression.

Intrinsic Sema3A expression is required for proper dorsal projection of MMCm neurons and fasciculation of LMC axons

The role of endogenous intrinsic Sema3A was further examined by silencing its mRNA with U6-based expression of small interfering RNA hairpins (pShSema3A-EGFP). The selected constructs could efficiently and specifically extinguish Sema3A in the ventral horn at stages up to HH25. By contrast, they did not interfere with Sema3C mRNA, which is closely related to Sema3A (see Fig. S1I in the supplementary material). Control

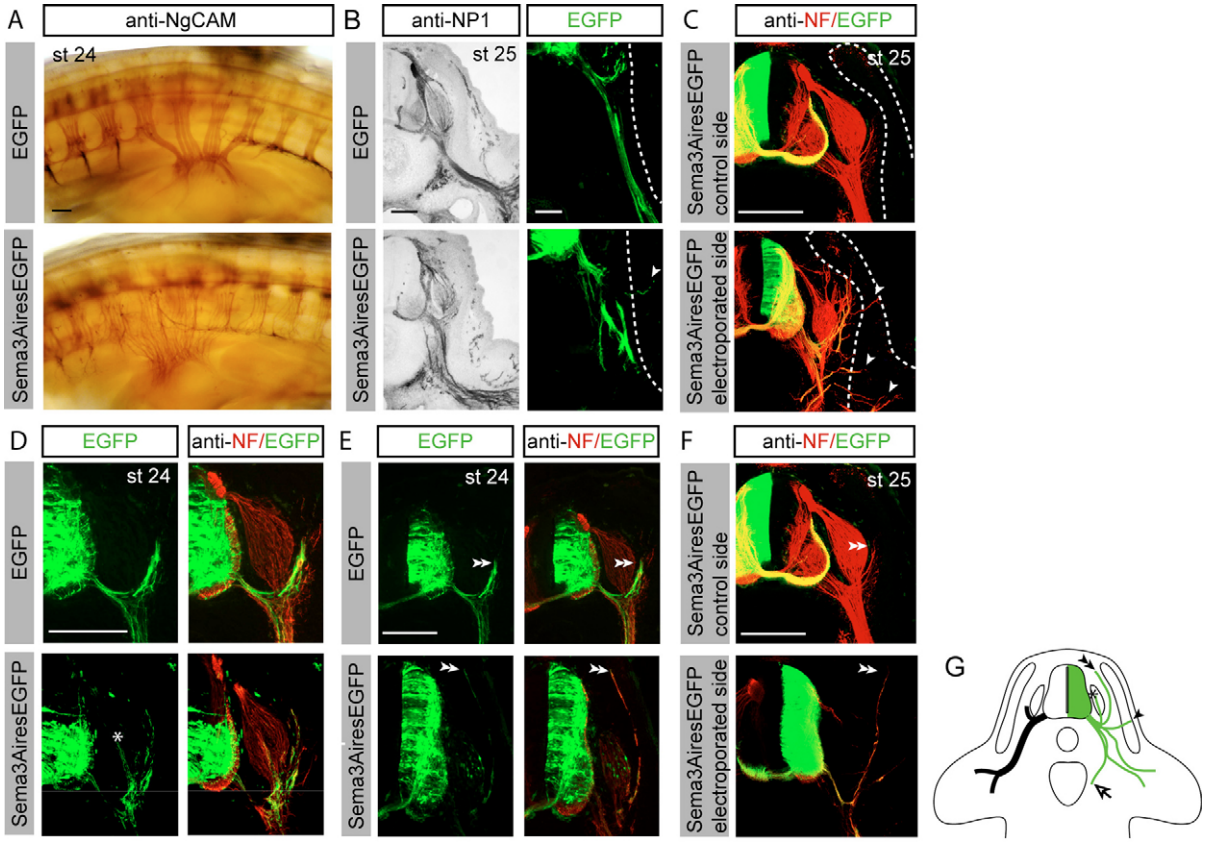

Fig. 2. Sema3A overexpression in motoneurons disrupts nerve projections. (**A-F**) Effects of control EGFP, Sema3AiresEGFP overexpression on spinal nerve fasciculation (A,B) , on motor projections (arrowhead, B,C) towards the dermamyotome (outlined), the DRG (asterisk, D), and on dorsal ramus length (E, double arrowhead). A shows NgCAM immunostaining on whole-mount HH24 embryos. Immunolabeling (indicated in horizontal frames) was performed on transverse cryostat sections (B,D,E) or on vibratome sections (C,F) and observed by confocal microscopy. Scale bars: 100 μm. (**G**) Schematic of the misrouting produced by Sema3A overexpression (defects, right side, in green; normal pattern, left side).

experiments were done with scrambled shRNA construct (pShScramble-EGFP; see Fig. S1I in the supplementary material). As revealed by measures on sections labeled with the NgCAM axonal marker, silencing of Sema3A in motoneurons significantly decreased the caliber of their ventral spinal nerves (Fig. 3B,C). This was not due to deficit of motoneurons and subsequent loss of axons, as demonstrated by TUNEL labeling and counting of Islet1/2$^+$ nuclei in the ventral horn of electroporated and control sides of pShSema3A-EGFP embryos (see Fig. S1J,K in the supplementary material). Rather the motor tracts appeared compacted, as illustrated by lateral observations of in toto NgCAM immunostaining (Fig. 3A).

Next, we investigated whether axonal misrouting could result from intrinsic Sema3A knockdown in motoneurons. Control MMCm neurons initially project towards the dermamyotome and then turn dorsally between the DRG and the dermamyotome (Gutman et al., 1993) by the time they endogenously express Sema3A (Fig. 1). In toto NgCAM immunostaining of spinal nerves in pShSema3A-EGFP embryos showed a reduction in the length of MMC fascicles extending from the electroporated side, compared with the control side (Fig. 3A). To confirm this observation, the length of MMC fibers was then measured on cryostat sections stained with anti-NF160kD. No significant difference was found in the length of pShSema3A-EGFP$^-$ fibers labeled with NF160kD between electroporated and non-electroporated sides. The length of NF$^+$/pShScramble-EGFP$^-$ and NF$^+$/pShSema3A-EGFP$^-$ fibers in the dorsal ramus was also similar (Fig. 3F). In order to eliminate inter-individual differences in fibers growth, we calculated the ratio of the length of pShSema3A-EGFP$^+$ or pShScramble-EGFP$^+$ fibers to that of NF$^+$/EGFP$^-$ fibers in the same ramus. pShSema3A-EGFP$^+$ axons were significantly shorter than pShScramble-EGFP$^+$ axons (Fig. 3D,E). In numerous cases, pShSema3A-EGFP$^+$ axons could turn dorsally but failed to further extend as control axons normally did (Fig. 3D). By contrast, no defect in the ventral trajectory of LMC axons could be seen, consistent with the absence of early intrinsic expression in this population of motoneurons. Intriguingly, although intermingled with pShSema3A-EGFP$^+$ neurons, pShSema3A-EGFP$^-$ MMC motoneurons properly extend their axons along the dorsal route, suggesting that intrinsic Sema3A acts through a cell-autonomous mechanism. Overall, Sema3A loss and gain of functions produce mirror phenotypes on spinal nerves, inhibition and exuberant growth of the dorsal ramus, hyperfasciculation and defasciculation of the ventral ramus, respectively.

Intrinsic Sema3A modulates growth cone responsiveness to environmental Sema3A

We hypothesized that fasciculation and pathfinding defects of spinal nerves induced by Sema3A misexpression in motoneurons resulted from changes of motor axon responsiveness to environmental guidance cues. Notably in the gain-of-function studies, motor axons extended in territories that express Sema3A and are normally not

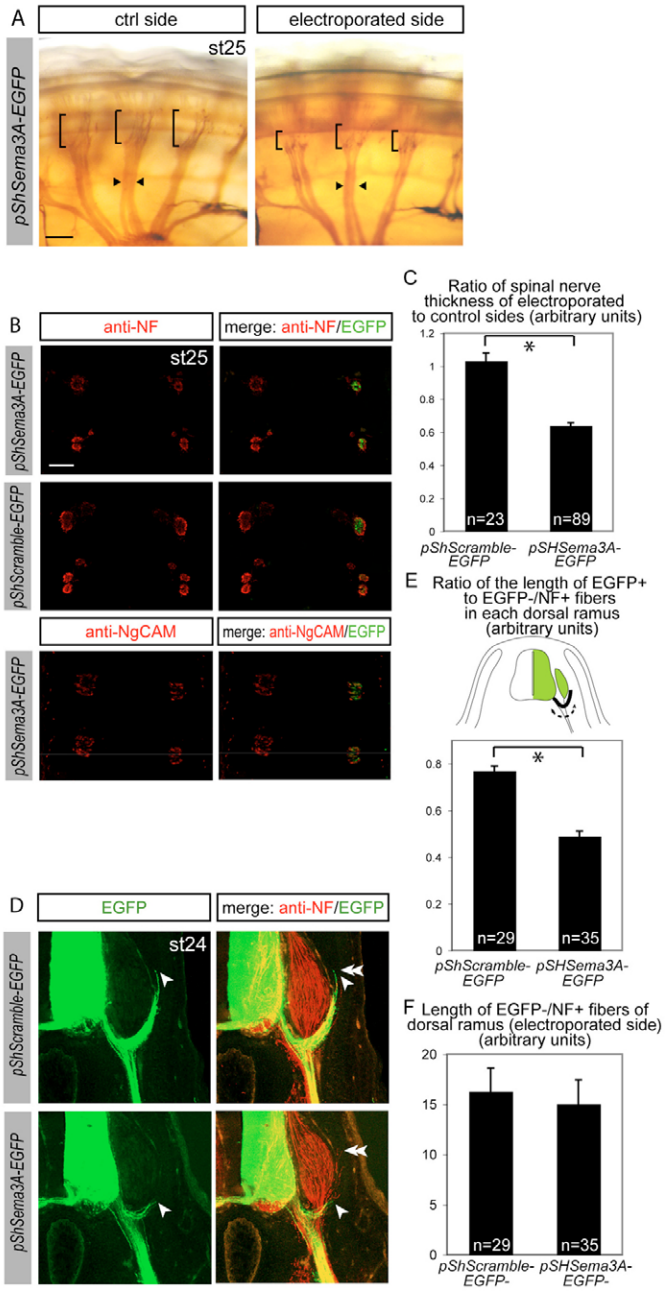

Fig. 3. In vivo Sema3A silencing in motoneurons alters motor axon tracts. (**A**) In toto NgCAM immunostaining (lateral view) on pShSema3A-EGFP embryo showing the reduction of MMC axon length (bracket) and ventral nerve thickness (arrowheads) on the electroporated side compared with the control side. (**B**) Horizontal cross sections at the cervical-brachial level of spinal nerves labeled with NF160kD or NgCAM from pShSema3A-EGFP or pShScramble-EGFP embryos. (**C**) Histogram of normalized spinal nerve thickness in control and pShSema3A-EGFP HH25 embryos (spinal nerve sections from three pShScramble-EGFP embryos and eight pShSema3A-EGFP embryos; *, $P<0.0001$ with Mann-Whitney test). (**D**) Transverse sections at the cervical-brachial level of pShSema3A-EGFP and pShScramble-EGFP HH24 embryos stained with NF160kD. (**E**) Histogram of the ratio of the length of EGFP$^+$ fibers to NF$^+$ fibers within the dorsal ramus, as illustrated (dorsal rami from five pShScramble-EGFP and seven pShSema3A-EGFP embryos; *, $P<0.0001$ with Mann-Whitney test). (**F**) Histogram of the length of NF$^+$/EGFP$^-$ fibers of dorsal rami in pShScramble and pShSema3A conditions (arbitrary units). Error bars indicate s.e.m. Scale bars: 100 μm.

permissive, and this prompted us to examine whether intrinsic Sema3A expression in motoneurons could modulate their own response to environmentally expressed Sema3A. To address this issue, the growth cone response of Sema3AiresEGFP$^+$ motoneurons to environmental Sema3A was analyzed in ex vivo collapse assays performed on ventral spinal cord explants from HH24 embryos after 24 hours culture (Fig. 4A). Exogenous Sema3A application caused the collapse of 75% and 77% of motoneuron growth cones from control EGFP$^+$ and non-electroporated explants, respectively (Fig. 4A). No difference in the general pattern of axon growth was observed between Sema3AiresEGFP$^+$ and control EGFP$^+$ explants (see Fig. S2 in the supplementary material). About 20% of axons emerging from explants were EGFP-positive in both control EGFP and Sema3AiresEGFP explants. Surprisingly, only 35% of

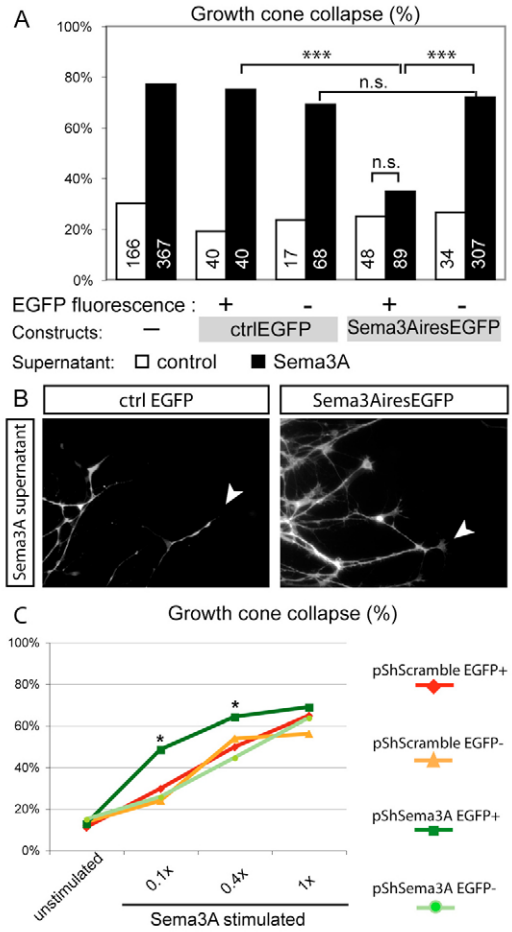

Fig. 4. Intrinsic Sema3A cell-autonomously sets the growth cone sensitivity to exogenous Sema3A. (**A**) Histogram showing the percentage of EGFP$^+$ or EGFP$^-$ collapsed growth cones of Sema3AiresEGFP or control EGFP ventral spinal cord explants following exposure to Sema3A or control supernatant. Axons were counted from at least three independent experiments. ***, $P<0.001$ with χ^2 test; n.s., non significant. (**B**) Morphology of ctrlEGFP$^+$ (collapsed) or Sema3AiresEGFP$^+$ (non-collapsed) axons emerging from ventral spinal cord explants after Sema3A supernatant exposure. (**C**) Comparison of the collapse response (%) of pShScramble-EGFP$^+$, pShScramble-EGFP$^-$, pShSema3A-EGFP$^+$ and pShSema3A-EGFP$^-$ axons following exposure to decreasing doses of Sema3A. *$P<0.01$ with χ^2 test between pShSema3A-EGFP$^+$ and all other conditions. At least 150 growth cones from two embryos were examined in each condition.

Sema3AiresEGFP$^+$ growth cones were collapsed by Sema3A, which was not significantly different from the level of basal collapse under control treatment (25%; Fig. 4A,B). Thus intrinsic Sema3A overexpression abrogates the growth cone collapse normally exerted by exogenous Sema3A.

Exposure to environmental Sema3A was shown to desensitize axons to further acute Sema3A treatment (Ming et al., 2002; Piper et al., 2005). Release of Sema3A by Sema3AiresEGFP$^+$ explants in the culture medium could result in general desensitization to Sema3A. We thus examined the response of Sema3AiresEGFP$^-$ motor axons growing from explants electroporated with Sema3AiresEGFP, as these axons were submitted to chronic Sema3A exposure. However, unlike Sema3AiresEGFP$^+$ axons, their level of collapse was as high as that of control motor axons (72%; Fig. 4A). Thus Sema3A overexpression in spinal explants antagonizes the repulsive effects of external Sema3A. Interestingly, in this experimental condition this process is not due to general desensitization following chronic exposure to Sema3A but is restricted to neurons overexpressing Sema3A.

These results suggest that endogenous Sema3A in motoneurons could limit growth cone responsiveness to environmental Sema3A, particularly by the time explants are submitted to collapse assays. We may thus expect Sema3A knockdown to increase the collapse response to Sema3A exposure. Since high dose of Sema3A induces more than 70% collapse in control motoneurons, we tested the effect of Sema3A silencing in motoneurons on their collapse response to decreasing doses of Sema3A supernatant. As the level of endogenous Sema3A may differ at different levels of the spinal cord, the percentages of collapse were determined from the systematic analysis of all ventral spinal cord explants derived from a restricted brachial region for two electroporated embryos. pShSema3A-EGFP electroporation did not affect axon outgrowth or growth cone morphology compared to control pShScramble-EGFP (see Fig. S2 in the supplementary material). Interestingly, 48.5% of pShSema3A-EGFP$^+$ axons were collapsed using a 0.1× dose of Sema3A supernatant, whereas only 29% of pShScramble-EGFP$^+$ were collapsed with the same dose (Fig. 4C). Similarly, the percentage collapse of pShSema3A-EGFP$^+$ axons was significantly higher than that of pShScramble-EGFP$^+$ ones using a 0.4× dose of Sema3A. By contrast, unstimulated pShScramble-EGFP$^+$ and pShSema3A-EGFP$^+$ growth cones displayed similar low levels of collapse (12% and 12.6% respectively). Thus Sema3A silencing in motoneurons enhances their responsiveness to external Sema3A. Moreover, pShSema3A-EGFP$^-$ axons display the same level of collapse as pShScramble-EGFP$^+$ and pShScramble-EGFP$^-$ axons in all tested conditions (Fig. 4C). This result indicates that endogenous Sema3A expression in pShSema3A-EGFP$^-$ neurons decreases the sensitivity of their axons to environmental Sema3A but not of the neighboring pShSema3A-EGFP$^+$ axons. This further supports the idea that motoneuronal Sema3A modulates growth cone responsiveness through a cell autonomous pathway.

Intrinsic Sema3A downregulates Nrp1 availability at the growth cone surface

One possibility that could explain the loss of response was that Sema3A expression in motoneurons modulates the response to external Sema3A. First, we examined the expression of the Sema3A receptor Nrp1 (He and Tessier-Lavigne, 1997; Kitsukawa et al., 1997; Kolodkin et al., 1997), by in situ hybridization on spinal cord sections from Sema3AiresEGFP embryos. No difference in the level of *Nrp1* transcripts could be detected between electroporated and control ventral horns (Fig. 5A) indicating that intrinsic Sema3A does not modulate Nrp1 expression at the transcriptional level. Second, we searched for a regulation of *Nrp1* at the protein level. The defasciculation state of Sema3AiresEGFP$^+$ spinal nerves limited comparative quantification of Nrp1 labeling on motor axons. Thus Nrp1 immunolabeling was analyzed in separated growth cones from explant cultures. The total pool of Nrp1 was immunolabeled after membrane permeabilization and quantified (Fig. 5B,D). Similar amounts of Nrp1 were measured in Sema3AiresEGFP$^+$, Sema3AiresEGFP$^-$ and control EGFP$^+$ growth cones indicating that the protein is correctly sorted to axon terminals.

Third, another possibility could be that Sema3A modifies the availability of Nrp1 at the surface of the growth cone. We thus addressed this hypothesis by immunolabeling Nrp1 in non-permeabilized conditions (Fig. 5C). Notably, while the intensity of the NgCAM marker was constant (Fig. 5F), Nrp1 expression was significantly reduced by 43% in Sema3AiresEGFP$^+$ growth cones compared with EGFP controls (Fig. 5E). Furthermore, such reduction was not detected in Sema3AiresEGFP$^-$ growth cones, consistent with a local regulatory mechanism (Fig. 5C,E). If Sema3A decreases the Nrp1 level then its knockdown in motoneurons would be expected to result in the opposite effect. Consistent with this hypothesis, silencing of Sema3A in pShSema3A-EGFP$^+$ motor growth cones led to significant increase of Nrp1 surface labeling when compared with pShSema3A-EGFP$^-$ growth cones (Fig. 5G,H). These results indicated that the control of axon sensitivity, dependent on intrinsic Sema3A, is exerted by local regulation of Nrp1 at the growth cone surface.

Our in vivo and ex vivo data suggested that Sema3A-dependent control of axon sensitivity and Nrp1 availability take place in neurons that express Sema3A. As Sema3A is a secreted protein, this control could rely on intracellular or autocrine mechanisms.

We first investigated the subcellular localization of Sema3A overexpressed in motoneurons in vivo. Myc-tagged Sema3A was detected in motoneuron somata but also along spinal nerves (Fig. 6A). Furthermore, anti-Myc immunostaining performed on Sema3AiresEGFP$^+$ explants in non-permeabilized conditions, detected Myc-Sema3A at the surface of motor axons (data not shown). These data thus indicated that Sema3A is present at the axon surface, which favored the hypothesis of an autocrine mechanism.

If true, the action of intrinsic Sema3A may have been restricted to Sema3AiresEGFP$^+$ axons due to a limited amount of Sema3A secreted from the electroporated motoneurons. One way to test this hypothesis was to analyze whether higher levels of Sema3A overexpression in explants could affect both Sema3AiresEGFP$^-$ and Sema3AiresEGFP$^+$ axons ex vivo. Injected plasmid concentration was increased from 1.5 μg/μl to 2 μg/μl and electroporation parameters were modified to obtain about 60% of EGFP$^+$ axons emerging from Sema3AiresEGFP explants. We ensured that axon growth in these explants was still not altered compared to control explants.

In these conditions, the percentage of collapsed Sema3AiresEGFP$^-$ growth cones following treatment by Sema3A supernatant (60.3%) was significantly lower than that of control explant axons (80.8%; Fig. 6B), which suggested that large excess of Sema3A expression in explants could desensitize the growth cones through a paracrine pathway. Nevertheless, the desensitization was only partial as a significantly higher proportion of growth cones remained collapsed, compared with Sema3AireEGFP$^+$ ones (26.9%; Fig. 6B). This indicates that Sema3A-dependent desensitization preferentially affects Sema3A-overexpressing neurons. We next examined whether the decrease of axon sensitivity of

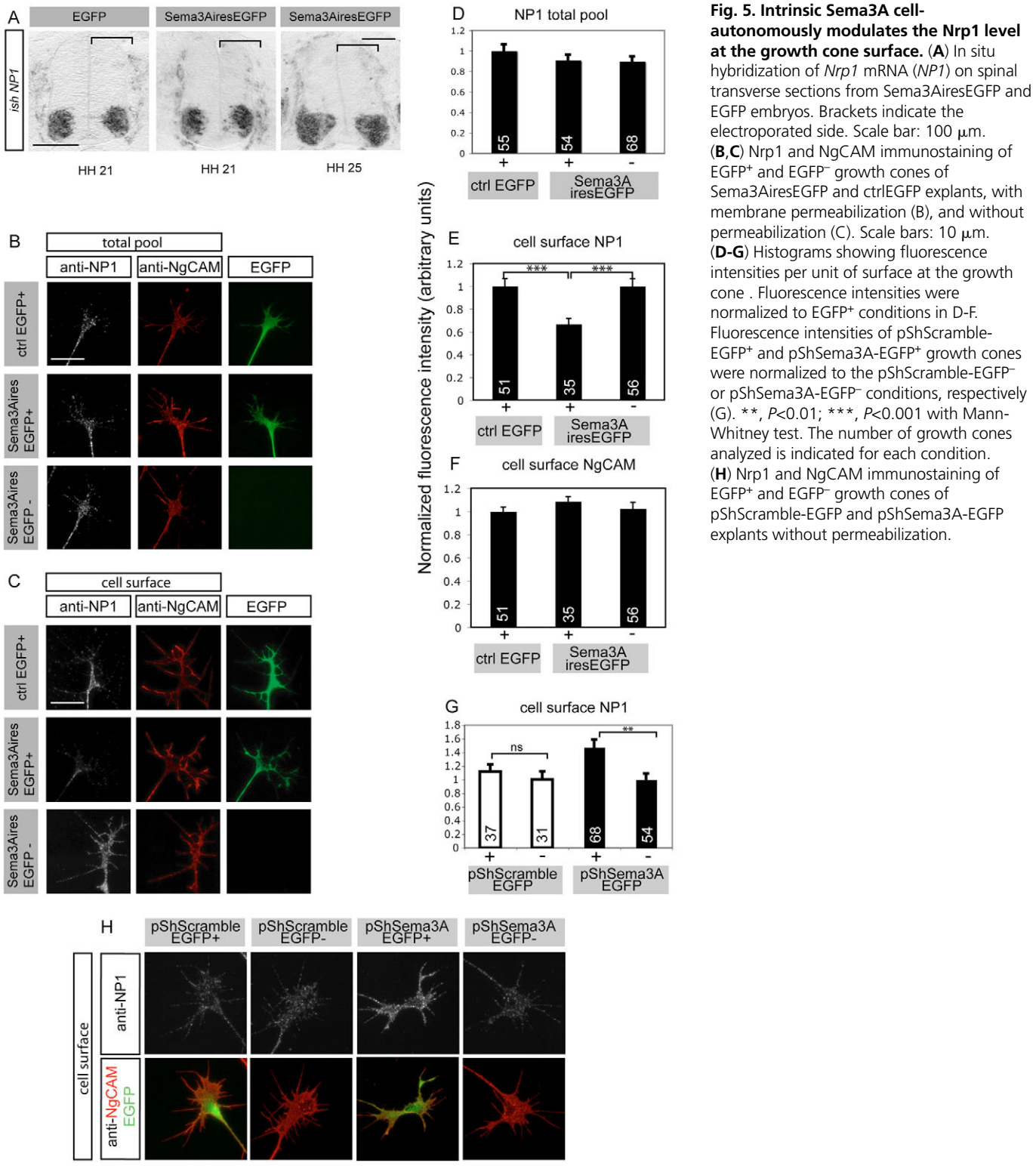

Fig. 5. Intrinsic Sema3A cell-autonomously modulates the Nrp1 level at the growth cone surface. (**A**) In situ hybridization of *Nrp1* mRNA (*NP1*) on spinal transverse sections from Sema3AiresEGFP and EGFP embryos. Brackets indicate the electroporated side. Scale bar: 100 μm. (**B**,**C**) Nrp1 and NgCAM immunostaining of EGFP$^+$ and EGFP$^-$ growth cones of Sema3AiresEGFP and ctrlEGFP explants, with membrane permeabilization (B), and without permeabilization (C). Scale bars: 10 μm. (**D-G**) Histograms showing fluorescence intensities per unit of surface at the growth cone . Fluorescence intensities were normalized to EGFP$^+$ conditions in D-F. Fluorescence intensities of pShScramble-EGFP$^+$ and pShSema3A-EGFP$^+$ growth cones were normalized to the pShScramble-EGFP$^-$ or pShSema3A-EGFP$^-$ conditions, respectively (G). **, P<0.01; ***, P<0.001 with Mann-Whitney test. The number of growth cones analyzed is indicated for each condition. (**H**) Nrp1 and NgCAM immunostaining of EGFP$^+$ and EGFP$^-$ growth cones of pShScramble-EGFP and pShSema3A-EGFP explants without permeabilization.

Sema3AiresEGFP$^-$ axons could be reflected in the amount of available Nrp1 in their growth cones. Interestingly and in contrast to that observed previously, the level of Nrp1 staining at the surface of Sema3AiresEGFP$^-$ was significantly reduced compared to control EGFP$^+$ axons (Fig. 6C,D). This suggested that Sema3A secreted by Sema3AiresEGFP$^+$ motoneurons can modulate Nrp1 expression at the growth cone in a paracrine manner. Nevertheless, and as observed in the collapse assays, Sema3A overexpression predominantly affects Nrp1 on Sema3AiresEGFP$^+$ growth cones (Fig. 6C,D).

Altogether these results support the hypothesis that neuronal Sema3A modulates growth cone sensitivity by controlling surface Nrp1 via a secretory pathway and through a predominantly autocrine mechanism.

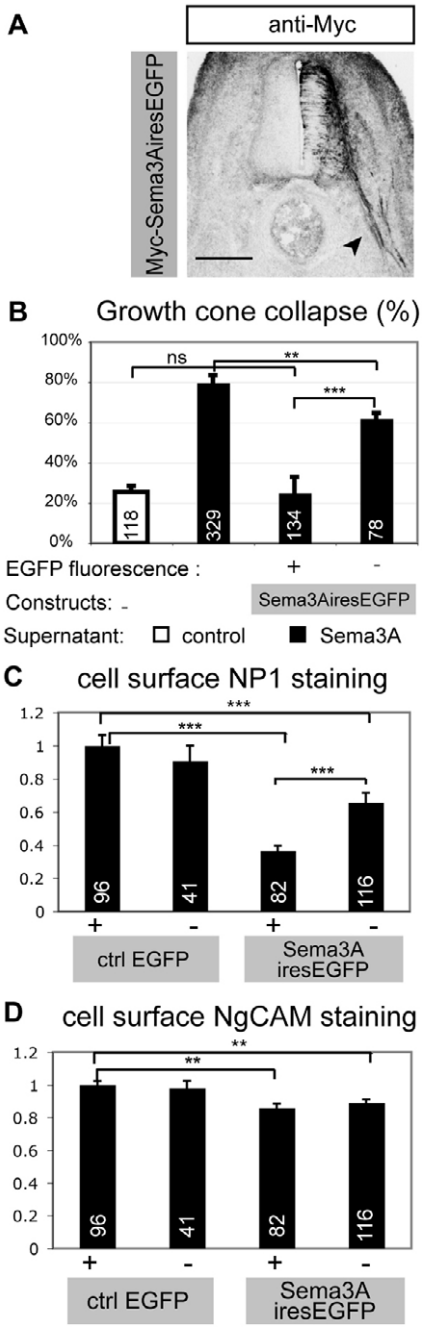

Fig. 6. Non cell-autonomous effects of motoneuronal Sema3A in conditions of forced overexpression suggests that intrinsic Sema3A acts via secretion. (**A**) Myc immunostaining on transverse sections of Sema3AiresEGFP HH25 embryo showing that Myc-tagged Sema3A is targeted to the defasciculated spinal nerve (arrowhead). (**B**) Histogram showing the percentage (±s.d.) of EGFP$^+$ or EGFP$^-$ collapsed growth cones following Sema3A and control supernatant exposure, of Sema3AiresEGFP, or control ventral spinal cord explants. **, P<0.01; ***, P<0.001 with Student's t-test; n.s.: non significant. The total number of axons from three independent experiments is indicated on the bars. (**C**,**D**) Histograms showing Nrp1 (NP1) and NgCAM immunofluorescence intensities per unit of surface at the growth cone in conditions of increased level of Sema3A overexpression. Immunolabeling of cell surface Nrp1 and NgCAM was performed on non-permeabilized explants. Fluorescence intensities were normalized to EGFP$^+$ conditions. **, P<0.01; ***, P<0.001 with Mann-Whitney test. The number of axons examined is indicated on the bars.

DISCUSSION

This work reveals a novel mechanism by which neurons express Sema3A to set the sensitivity of their growth cones to environmental Sema3A, thereby regulating their pathway choices. This regulation occurs post-transcriptionally through the local control of available Nrp1 receptor at the growth cone surface.

Our data suggest that this regulation concerns neurons intrinsically expressing Sema3A. Such role for class III semaphorins was unexpected because these cues were so far implicated in axon guidance as chemotropic intercellular signals (Raper, 2000). First, in vivo observations showed that the reduction of motor projections along the dorsal route affected MMC neurons in which Sema3A was knockdown but not those that escaped the silencing, even though both were mixed together in the ventral horn and their axons not segregated. Second, in ex vivo gain-of-function experiments producing limited Sema3A overexpression, the desensitization and reduction of Nrp1 level was only affected in electroporated motoneurons. Similarly, increased collapse response and Nrp1 level induced by knockdown of Sema3A were both restricted to neurons in which Sema3A was silenced. However, Sema3A was detected at the surface of motor axons both in vivo and in vitro, indicating that Sema3A might be secreted and retained along the axon shaft, as reported in previous work (de Wit et al., 2005). Increasing the level of Sema3A overexpression was sufficient to expand the effect to the population of non-electroporated motoneurons. The desensitization might thus occur through Sema3A secretion, and the cell-autonomous nature of the effect might be due to limited diffusion of the cue (Fig. 7A). In physiological contexts, an autocrine loop might be the predominant pathway by which neuronal Sema3A sets the sensitivity of the growth cones to environmental Sema3A, although paracrine effects cannot be formally excluded. Future studies will address this issue with tools designed for interfering with the diffusion of the cue in vivo.

This work provides the first evidence that motoneuronal SemaIIIs play a critical role in spinal nerve pathfinding. Previous studies demonstrated that repulsive signaling by environmental SemaIII expression in peripheral tissues is crucial for axon pathway choices and fasciculation (Huber et al., 2005; Kitsukawa et al., 1997; Varela-Echavarria et al., 1997). In particular, analysis of genetic disruption of Nrp1-Sema3A signaling in mouse models resulted in defasciculation of motor axons (Huber et al., 2005; Kitsukawa et al., 1997). Intriguingly, our work reveals that targeted Sema3A overexpression in motoneurons also induces a strong spinal nerve defasciculation and exuberant motor axon outgrowth in normally non-permissive territories. Conversely, targeted Sema3A loss of function in motoneurons induced mirror phenotypes, with motor axons being compacted and their growth along the dorsal route inhibited. These results show that motoneuronal SemaIIIs are also major determinants of motor axon pathfinding.

Our data indicate a novel guidance model in which intrinsic Sema3A regulates axon responsiveness to its environmental counterpart. In vitro, Sema3A overexpression in motoneurons reduced the sensitivity of their axons to exogenous sources of Sema3A whereas Sema3A silencing had the opposite effect. This modulation of responsiveness was correlated with decrease and increase of Nrp1 surface level in gain and loss of function, respectively. By strengthening or relaxing the repulsive forces emanating from non-permissive territories, Sema3A in motoneurons might thus set Nrp1 levels to provide the appropriate level of surrounding repulsion over axon navigation. It is not technically possible to compare Sema3A-induced collapse responses of LMC and MMC motoneurons at early stages when only MMC

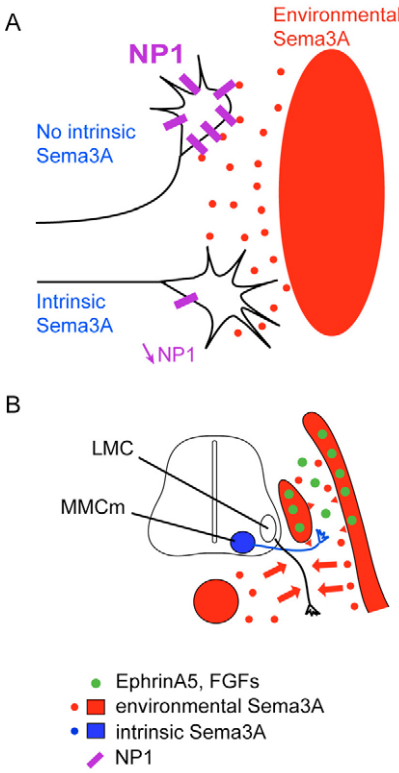

Fig. 7. Model of action of intrinsic Sema3A. (**A**) Mode of action of intrinsic Sema3A, showing that Sema3A expressed in neurons inhibits the response of their growth cones to environmental Sema3A through regulation of cell availability of Nrp1 (NP1). Predominant autocrine effect of neuronal semaphorin is indicated with an arrow. (**B**) Mechanism of interplay between intrinsic and extrinsic Sema3A in the development of motoneuron projections. Nrp1^{+} LMC axons are guided ventrally by the repulsive effects of Sema3A expressed in the DRG, the notochord and the dermamyotome. MMC axons are attracted dorsally by cues including ephrinA5 and FGFs. Intrinsic Sema3A in Nrp1 $^{+}$ MMCm neurons decreases their sensitivity to environmental repulsion by Sema3A, which enables their axons to project dorsally but to avoid the DRG and the dermamyotome.

motoneurons express Sema3A. Moreover, heterogeneous level of Sema3A expression among motoneurons complicates the analysis of growth cone behaviors in culture assays. This issue should be addressed by using specific knock-in mouse models. Nevertheless, the present work already suggests that differential expression of Sema3A in motoneuron columns may reflect a requirement for distinct levels of repulsive constraints along the ventrolateral and dorsal routes. The trajectory of LMC axons is directed towards a downhill Sema3A gradient, generated by combined dorsolateral and ventromedial Sema3A sources (Huber et al., 2005; Kitsukawa et al., 1997; Varela-Echavarria et al., 1997). Lack of early Sema3A expression in LMC neurons may thus potentiate the surround repulsion to properly channel the tract (Fig. 7B). By contrast, MMC axons exiting the ventral horn are segregated from LMC axons and dorsally oriented by the chemoattractants ephrin-A5 and FGF (Eberhart et al., 2004; Shirasaki et al., 2006). This dorsal route forces MMC axons to grow towards an uphill Sema3A repulsive gradient produced by the DRG and the dermamyotome. Weakening these repulsive forces by Sema3A expression in MMC neurons could thus permit or facilitate the extension of their axons along the dorsal route (Fig. 7B). The dynamic expression pattern of intrinsic Sema3A could also contribute to modulate growth cone behaviors to Sema3A sources during axon navigation. Interestingly at later stages, Sema3A is activated in LMC neurons when their axons reach the plexus, defasciculate and re-arrange according to their pool identity to invade the limb, where Sema3A is produced. Such intrinsic expression could facilitate the reorganization of motor fibers, their ingrowth in the limb and the topographic selection of target muscles, by modulating environmental repulsive forces.

Other mechanisms could also contribute to generate the phenotypes that we observed. First, defasciculation of spinal nerves following Sema3A overexpression in motoneurons could result from contact-mediated axo-axonal repulsion due to the local presentation of Sema3A along the axon shaft, as proposed for the transmembrane Sema1a in *Drosophila* (Yu et al., 2000). However, in explant cultures, Sema3AiresEGFP^{+} and Sema3AiresEGFP^{-} axons, both of which expressing Nrp1, were often associated or in close proximity. Moreover, segregation of these axons into distinct fascicles was not observed in vivo (data not shown). Second, by reducing the level of Nrp1, overexpressed Sema3A could alter axon adhesiveness thus leading to defasciculation of motor axon tracts, but this is, however, unlikely to be responsible for other prominent phenotypes associated with Sema3A loss and gain of function, such as aberrant growth within the dermamyotome and the notochord, or the inhibition of MMC axon growth along the dorsal route resulting from Sema3A silencing. Finally, altered migration of motoneurons could account for some of the defects observed. Motoneuron-derived semaphorins could indeed be also required for the migration and aggregation of motoneurons in the ventral horn. Mispositioning of motoneurons induced by gain or loss of Sema3A, could then contribute to abnormal patterns of their axonal projections, particularly MMC neurons since Sema3A knockdown resulted in a reduced dorsal ramus. Analysis of motoneuron migration and settling with specific markers of motor pools in loss and gain of function experiments should solve this question.

The role of intrinsic Sema3A is unlikely limited to switching on and off the axon response. Rather, analysis of motoneuron behaviors having different levels of Sema3A, achieved through gain and loss of function approaches, strongly support the idea that intrinsic Sema3A enables a range of sensitivity to environmental repulsive constraints to be generated. In the collapse assays, motoneurons that had the highest Sema3A level had the lowest Nrp1 surface expression and were the least sensitive to exogenously applied Sema3A. In physiological contexts, this property might be used for modifying the strength of guidance cues and delineating accurate trajectories within gradients. The tight control of growth cone sensitivity, allowing local and reversible modulation of axon behaviors to continuously changing environments, emerges from several studies as a critical aspect of the specification of axon pathways. In the context of chemotropic guidance cues, PKA activation modifies the amount of the cell surface expression of DCC receptors, leading to modulation of growth cone responsiveness to netrins (Bouchard et al., 2004). However, factors upstream of this pathway are not known. Another example of receptor regulation was reported for Slit-Robo signaling (Keleman et al., 2002). However, this mechanism was shown to direct all-or-none responses to Slit rather than fine tuning of the sensitivity. The present work reveals an advantageous mechanism based on a single ligand-receptor pair, in which the display of the receptor and the growth cone sensitivity are both set by co-expression of the ligand. Interestingly, ligand-receptor co-expression has already been reported for ephrin-Eph and Ig superfamily cell adhesion molecule families although these studies did not relate to diffusible cues such

as Sema3A but to transmembrane proteins (Brummendorf and Rathjen, 1996; Marquardt et al., 2005). Particular cis- and trans-interactions between ephrin and Eph were found to abrogate axon responsiveness, by modulating ligand-induced intracellular signaling cascades (Carvalho et al., 2006; Hornberger et al., 1999). Fine tuning of growth cone sensitivity may thus be a fundamental feature of axon guidance shared by various cues even though it relies on different molecular pathways.

A series of recent works using genetic approaches in *Drosophila* reported a crucial role of the neuronal expression of the transmembrane Semaphorin 1a during the development of neuronal topographic projections. In the olfactory system, graded Sema1a among olfactory receptor neurons organize, through a non autonomous mechanism, axo-axonal contacts that are crucial for glomeruli target selection (Lattemann et al., 2007; Sweeney et al., 2007). Moreover, graded Sema1A is also cell-autonomously utilized by olfactory projection neurons and photoreceptor to specify the topography of their dendritic and axonal projections (Cafferty et al., 2006; Komiyama et al., 2007). Despite the fundamental differences between transmembrane and secreted semaphorins, our present finding suggests that the roles of neuronal semaphorins during axon development might be conserved in vertebrates.

Mechanisms that regulate Sema3A expression in motoneurons remain unknown. Combinations of transcription factors both control the topographic arrangement of spinal motoneurons into spatially and functionally distinct pools and their specific connectivity (Dasen et al., 2005; Kania et al., 2000; Tsuchida et al., 1994). A limited number of guidance receptors were found downstream of this transcriptional code (Kania and Jessell, 2003; Shirasaki and Pfaff, 2002). Interestingly, distinct pools of cranial and spinal motoneurons have been found to express specific combinations of semaphorins (Chilton and Guthrie, 2003; Cohen et al., 2005). Our functional data suggest that these cues are effectors by which the transcriptional program is executed. Moreover, peripheral signals encountered by navigating motor axons, including Sema3A could also regulate semaphorin expression in motoneurons, possibly acting through retrograde signaling.

Finally, SemaIIIs and neuropilins are widely expressed in the developing and adult organism, and are also associated with various pathological conditions such as tumorigenesis and axon regeneration. Regulation of the sensitivity to Sema3A may be of strong interest in these situations. In adults, spinal cord lesion has been shown both to induce Sema3A expression in glial scars, limiting axon regeneration (de Wit and Verhaagen, 2003) and to reactivate Sema3A in motoneurons (Lindholm et al., 2004). The latter could reflect an attempt to overcome scar-mediated inhibition. Intrinsic Sema3A expression to antagonize environmental Sema3A repulsion may thus represent a new therapeutic target. Coexpression of SemaIIIs and neuropilins has also been noted in several cases in cancer cells. Promising areas of future investigation will also be to determine the role of the interplay between intrinsic and extrinsic SemaIIIs in cancer cell dissemination, as well as in angiogenesis. Finally, this study more widely questions the possibility that this regulatory pathway includes diffusible cues such as other guidance factors, morphogens or chemokines, involved in the patterning of the developing organism.

This work was supported by ATIP CNRS program, ANR Neuroscience, Association Française contre les Myopathies (AFM), Wings for Life Spinal Cord Research Fundation, Fondation pour la Recherche Médicale (FRM), Postdoctoral fellowship from AFM to F.M. We thank J. Raper for the kind gift of Sema3A constructs and S. Creuzet for helpful advices on chick electroporation.

Supplementary material

Supplementary material for this article is available at http://dev.biologists.org/cgi/content/full/134/24/4491/DC1

References

Behar, O., Golden, J. A., Mashimo, H., Schoen, F. J. and Fishman, M. C. (1996). Semaphorin III is needed for normal patterning and growth of nerves, bones and heart. *Nature* **383**, 525-528.

Bouchard, J. F., Moore, S. W., Tritsch, N. X., Roux, P. P., Shekarabi, M., Barker, P. A. and Kennedy, T. E. (2004). Protein kinase A activation promotes plasma membrane insertion of DCC from an intracellular pool: A novel mechanism regulating commissural axon extension. *J. Neurosci.* **24**, 3040-3050.

Brummendorf, T. and Rathjen, F. G. (1996). Structure/function relationships of axon-associated adhesion receptors of the immunoglobulin superfamily. *Curr. Opin. Neurobiol.* **6**, 584-593.

Cafferty, P., Yu, L., Long, H. and Rao, Y. (2006). Semaphorin-1a functions as a guidance receptor in the Drosophila visual system. *J. Neurosci.* **26**, 3999-4003.

Carvalho, R. F., Beutler, M., Marler, K. J., Knoll, B., Becker-Barroso, E., Heintzmann, R., Ng, T. and Drescher, U. (2006). Silencing of EphA3 through a cis interaction with ephrinA5. *Nat. Neurosci.* **9**, 322-330.

Chilton, J. K. and Guthrie, S. (2003). Cranial expression of class 3 secreted semaphorins and their neuropilin receptors. *Dev. Dyn.* **228**, 726-733.

Cohen, S., Funkelstein, L., Livet, J., Rougon, G., Henderson, C. E., Castellani, V. and Mann, F. (2005). A semaphorin code defines subpopulations of spinal motor neurons during mouse development. *Eur. J. Neurosci.* **21**, 1767-1776.

Creuzet, S., Couly, G., Vincent, C. and Le Douarin, N. M. (2002). Negative effect of Hox gene expression on the development of the neural crest-derived facial skeleton. *Development* **129**, 4301-4313.

Dasen, J. S., Tice, B. C., Brenner-Morton, S. and Jessell, T. M. (2005). A Hox regulatory network establishes motor neuron pool identity and target-muscle connectivity. *Cell* **123**, 477-491.

de Wit, J. and Verhaagen, J. (2003). Role of semaphorins in the adult nervous system. *Prog. Neurobiol.* **71**, 249-267.

de Wit, J., De Winter, F., Klooster, J. and Verhaagen, J. (2005). Semaphorin 3A displays a punctate distribution on the surface of neuronal cells and interacts with proteoglycans in the extracellular matrix. *Mol. Cell. Neurosci.* **29**, 40-55.

Eberhart, J., Barr, J., O'Connell, S., Flagg, A., Swartz, M. E., Cramer, K. S., Tosney, K. W., Pasquale, E. B. and Krull, C. E. (2004). Ephrin-A5 exerts positive or inhibitory effects on distinct subsets of EphA4-positive motor neurons. *J. Neurosci.* **24**, 1070-1078.

Falk, J., Bechara, A., Fiore, R., Nawabi, H., Zhou, H., Hoyo-Becerra, C., Bozon, M., Rougon, G., Grumet, M., Puschel, A. W. et al. (2005). Dual functional activity of semaphorin 3B is required for positioning the anterior commissure. *Neuron* **48**, 63-75.

Feiner, L., Koppel, A. M., Kobayashi, H. and Raper, J. A. (1997). Secreted chick semaphorins bind recombinant neuropilin with similar affinities but bind different subsets of neurons in situ. *Neuron* **19**, 539-545.

Gavrieli, Y., Sherman, Y. and Ben-Sasson, S. A. (1992). Identification of programmed cell death in situ via specific labeling of nuclear DNA fragmentation. *J. Cell Biol.* **119**, 493-501.

Gutman, C. R., Ajmera, M. K. and Hollyday, M. (1993). Organization of motor pools supplying axial muscles in the chicken. *Brain Res.* **609**, 129-136.

Hamburger, V. and Hamilton, H. L. (1992). A series of normal stages in the development of the chick embryo. 1951. *Dev. Dyn.* **195**, 231-272.

He, Z. and Tessier-Lavigne, M. (1997). Neuropilin is a receptor for the axonal chemorepellent Semaphorin III. *Cell* **90**, 739-751.

Hornberger, M. R., Dutting, D., Ciossek, T., Yamada, T., Handwerker, C., Lang, S., Weth, F., Huf, J., Wessel, R., Logan, C. et al. (1999). Modulation of EphA receptor function by coexpressed ephrinA ligands on retinal ganglion cell axons. *Neuron* **22**, 731-742.

Huber, A. B., Kania, A., Tran, T. S., Gu, C., De Marco Garcia, N., Lieberam, I., Johnson, D., Jessell, T. M., Ginty, D. D. and Kolodkin, A. L. (2005). Distinct roles for secreted semaphorin signaling in spinal motor axon guidance. *Neuron* **48**, 949-964.

Kania, A. and Jessell, T. M. (2003). Topographic motor projections in the limb imposed by LIM homeodomain protein regulation of ephrin-A:EphA interactions. *Neuron* **38**, 581-596.

Kania, A., Johnson, R. L. and Jessell, T. M. (2000). Coordinate roles for LIM homeobox genes in directing the dorsoventral trajectory of motor axons in the vertebrate limb. *Cell* **102**, 161-173.

Keleman, K., Rajagopalan, S., Cleppien, D., Teis, D., Paiha, K., Huber, L. A., Technau, G. M. and Dickson, B. J. (2002). Comm sorts robo to control axon guidance at the Drosophila midline. *Cell* **110**, 415-427.

Kitsukawa, T., Shimizu, M., Sanbo, M., Hirata, T., Taniguchi, M., Bekku, Y., Yagi, T. and Fujisawa, H. (1997). Neuropilin-semaphorin III/D-mediated chemorepulsive signals play a crucial role in peripheral nerve projection in mice. *Neuron* **19**, 995-1005.

Kolodkin, A. L., Levengood, D. V., Rowe, E. G., Tai, Y. T., Giger, R. J. and Ginty, D. D. (1997). Neuropilin is a semaphorin III receptor. *Cell* **90**, 753-762.

Komiyama, T., Sweeney, L. B., Schuldiner, O., Garcia, K. C. and Luo, L. (2007). Graded expression of semaphorin-1a cell-autonomously directs dendritic targeting of olfactory projection neurons. *Cell* **128**, 399-410.
Lattemann, M., Zierau, A., Schulte, C., Seidl, S., Kuhlmann, B. and Hummel, T. (2007). Semaphorin-1a controls receptor neuron-specific axonal convergence in the primary olfactory center of Drosophila. *Neuron* **53**, 169-184.
Lin, W., Sanchez, H. B., Deerinck, T., Morris, J. K., Ellisman, M. and Lee, K. F. (2000). Aberrant development of motor axons and neuromuscular synapses in erbB2-deficient mice. *Proc. Natl. Acad. Sci. USA* **97**, 1299-1304.
Lindholm, T., Skold, M. K., Suneson, A., Carlstedt, T., Cullheim, S. and Risling, M. (2004). Semaphorin and neuropilin expression in motoneurons after intraspinal motoneuron axotomy. *NeuroReport* **15**, 649-654.
Luo, Y., Shepherd, I., Li, J., Renzi, M. J., Chang, S. and Raper, J. A. (1995). A family of molecules related to collapsin in the embryonic chick nervous system. *Neuron* **14**, 1131-1140.
Marquardt, T., Shirasaki, R., Ghosh, S., Andrews, S. E., Carter, N., Hunter, T. and Pfaff, S. L. (2005). Coexpressed EphA receptors and ephrin-A ligands mediate opposing actions on growth cone navigation from distinct membrane domains. *Cell* **121**, 127-139.
Marthiens, V., Gavard, J., Padilla, F., Monnet, C., Castellani, V., Lambert, M. and Mege, R. M. (2005). A novel function for cadherin-11 in the regulation of motor axon elongation and fasciculation. *Mol. Cell. Neurosci.* **28**, 715-726.
Melendez-Herrera, E. and Varela-Echavarria, A. (2006). Expression of secreted semaphorins and their receptors in specific neuromeres, boundaries, and neuronal groups in the developing mouse and chick brain. *Brain Res.* **1067**, 126-137.
Ming, G. L., Wong, S. T., Henley, J., Yuan, X. B., Song, H. J., Spitzer, N. C. and Poo, M. M. (2002). Adaptation in the chemotactic guidance of nerve growth cones. *Nature* **417**, 411-418.
Moret, F., Guilland, J. C., Coudouel, S., Rochette, L. and Vernier, P. (2004). Distribution of tyrosine hydroxylase, dopamine, and serotonin in the central nervous system of amphioxus (Branchiostoma lanceolatum): implications for the evolution of catecholamine systems in vertebrates. *J. Comp. Neurol.* **468**, 135-150.
Piper, M., Salih, S., Weinl, C., Holt, C. E. and Harris, W. A. (2005). Endocytosis-dependent desensitization and protein synthesis-dependent resensitization in retinal growth cone adaptation. *Nat. Neurosci.* **8**, 179-186.
Puschel, A. W., Adams, R. H. and Betz, H. (1995). Murine semaphorin D/collapsin is a member of a diverse gene family and creates domains inhibitory for axonal extension. *Neuron* **14**, 941-948.
Raper, J. A. (2000). Semaphorins and their receptors in vertebrates and invertebrates. *Curr. Opin. Neurobiol.* **10**, 88-94.
Shirasaki, R. and Pfaff, S. L. (2002). Transcriptional codes and the control of neuronal identity. *Annu. Rev. Neurosci.* **25**, 251-281.
Shirasaki, R., Lewcock, J. W., Lettieri, K. and Pfaff, S. L. (2006). FGF as a target-derived chemoattractant for developing motor axons genetically programmed by the LIM code. *Neuron* **50**, 841-853.
Sweeney, L. B., Couto, A., Chou, Y. H., Berdnik, D., Dickson, B. J., Luo, L. and Komiyama, T. (2007). Temporal target restriction of olfactory receptor neurons by Semaphorin-1a/PlexinA-mediated axon-axon interactions. *Neuron* **53**, 185-200.
Taniguchi, M., Yuasa, S., Fujisawa, H., Naruse, I., Saga, S., Mishina, M. and Yagi, T. (1997). Disruption of semaphorin III/D gene causes severe abnormality in peripheral nerve projection. *Neuron* **19**, 519-530.
Tsuchida, T., Ensini, M., Morton, S. B., Baldassare, M., Edlund, T., Jessell, T. M. and Pfaff, S. L. (1994). Topographic organization of embryonic motor neurons defined by expression of LIM homeobox genes. *Cell* **79**, 957-970.
Varela-Echavarria, A., Tucker, A., Puschel, A. W. and Guthrie, S. (1997). Motor axon subpopulations respond differentially to the chemorepellents netrin-1 and semaphorin D. *Neuron* **18**, 193-207.
Yaginuma, H., Tomita, M., Takashita, N., McKay, S. E., Cardwell, C., Yin, Q. W. and Oppenheim, R. W. (1996). A novel type of programmed neuronal death in the cervical spinal cord of the chick embryo. *J. Neurosci.* **16**, 3685-3703.
Yu, H. H., Huang, A. S. and Kolodkin, A. L. (2000). Semaphorin-1a acts in concert with the cell adhesion molecules fasciclin II and connectin to regulate axon fasciculation in Drosophila. *Genetics* **156**, 723-731.
Yu, T. W. and Bargmann, C. I. (2001). Dynamic regulation of axon guidance. *Nat. Neurosci.* **4**, 1169-1176.